# Supporting Information for "Comparison of Four Competing Invasion Percolation Models for Gas Flow in Porous Media"

I. Banerjee[1], A. Guthke[2], C.J.C. Van De Ven[3], K.G. Mumford[4], W. Nowak[1]

[1]Institute for Modelling Hydraulic and Environmental Systems (IWS)/LS3, University of Stuttgart, Germany

[2]Stuttgart Center for Simulation Science, Cluster of Excellence EXC 2075, University of Stuttgart, Stuttgart, Germany

[3]Department of Civil and Environmental Engineering, Carleton University, Ontario, Canada

[4]Department of Civil Engineering, Queen's University, Kingston, Canada

## Contents of this file

1. Figures S1 to S13

## Introduction

We present more visual evidence from our analyses supporting our results and conclusions. Figure S1 contains the experimental images and their blurred versions for experiments 10-B, 100-B and 250-B. Figure S2 contains the experimental images and their blurred versions for experiments 10-C, 100-C and 250-C. This is followed by corresponding best-fitting model realizations obtained using the maximum Jaccard coefficient for these experiments (Figures S3 and S4).

---

Corresponding author: Ishani Banerjee, Institute for Modelling Hydraulic and Environmental Systems (IWS)/LS3, University of Stuttgart, Germany. (ishani.banerjee@iws.uni-stuttgart.de)

The best-fitting model realizations to the experimental triplicate at 10 ml/min, 100 ml/min, and 250 ml/min, obtained using the maximum Diffused Jaccard coefficient (low) metric, are shown in Figures S5 - S7.

Figures S8 - S10 contain the best-fitting model realizations to the experimental triplicate at 10 ml/min, 100 ml/min, and 250 ml/min, obtained using the maximum Diffused Jaccard coefficient (med) metric.

The best-fitting model realizations to the experimental triplicate at 10 ml/min, 100 ml/min, and 250 ml/min, obtained using the maximum Diffused Jaccard coefficient (high) metric, are shown in Figures S11 - S13.

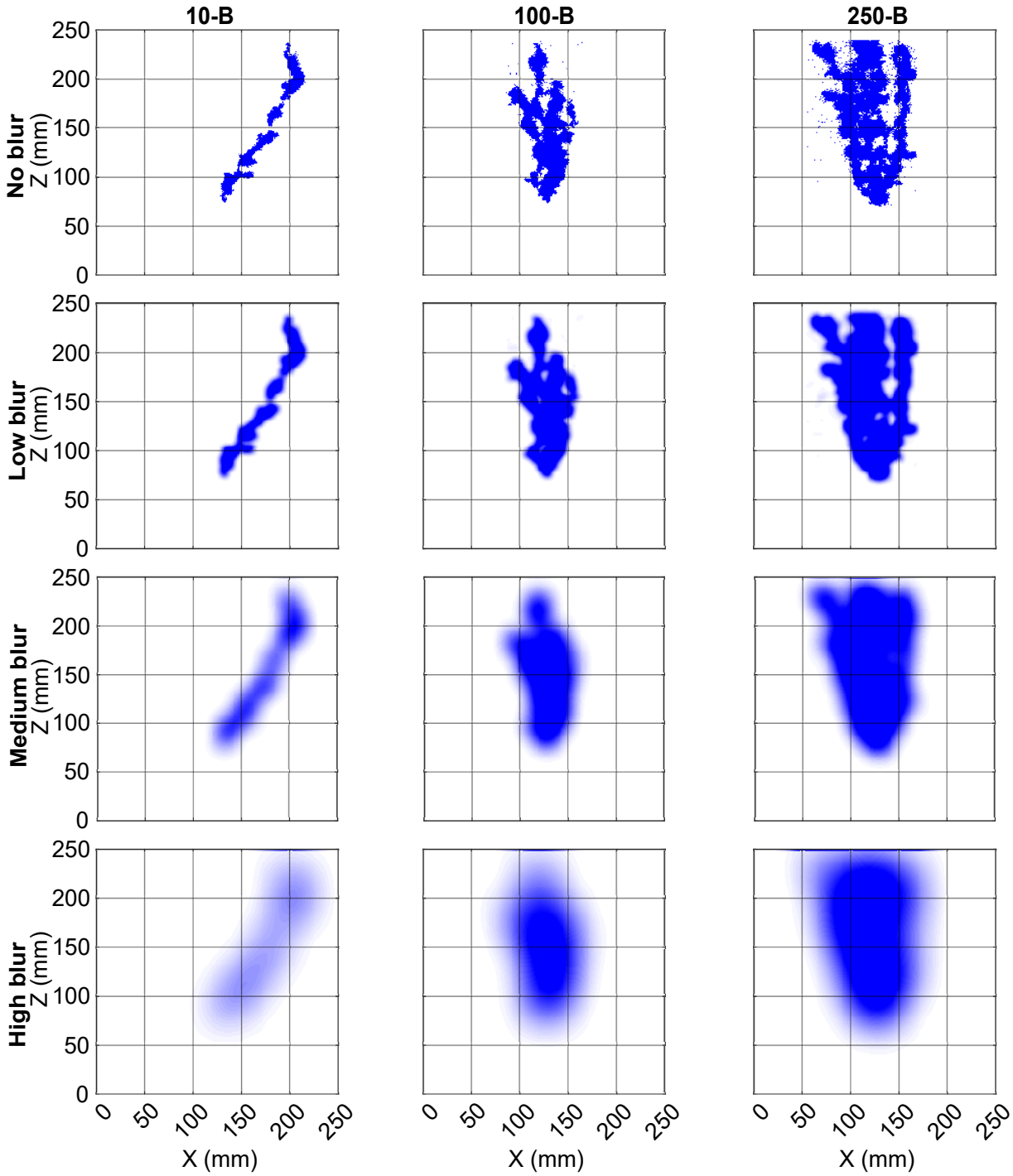


**Figure S1.** Final experimental image of the experiments 10-B, 100-B and 250-B. Row 2-4 contains the blurred version of the images of Row 1 for the three different blur-radii.

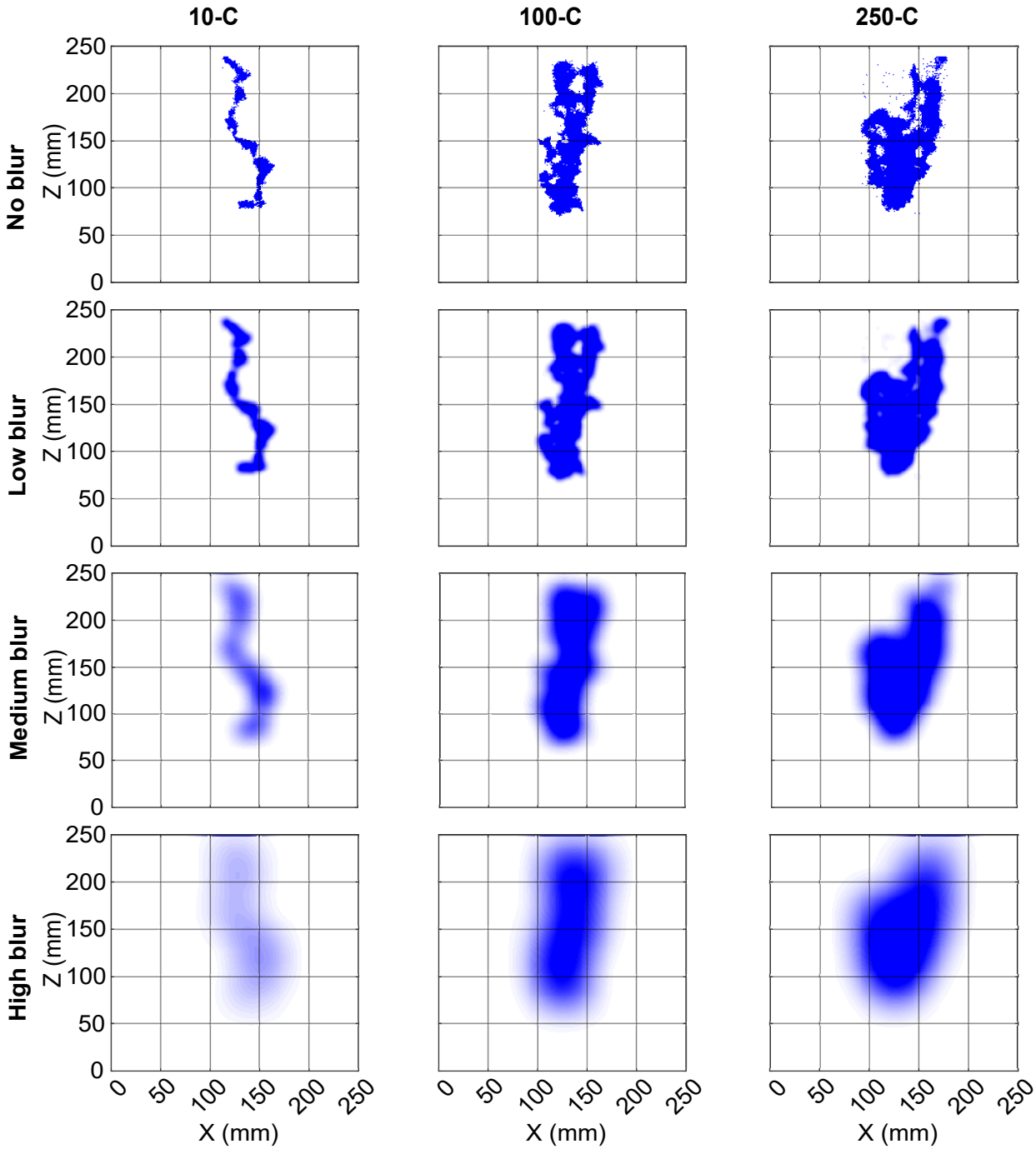


**Figure S2.** Final experimental image of the experiments 10-C, 100-C and 250-C. Row 2-4 contains the blurred version of the images of Row 1 for the three different blur-radii.

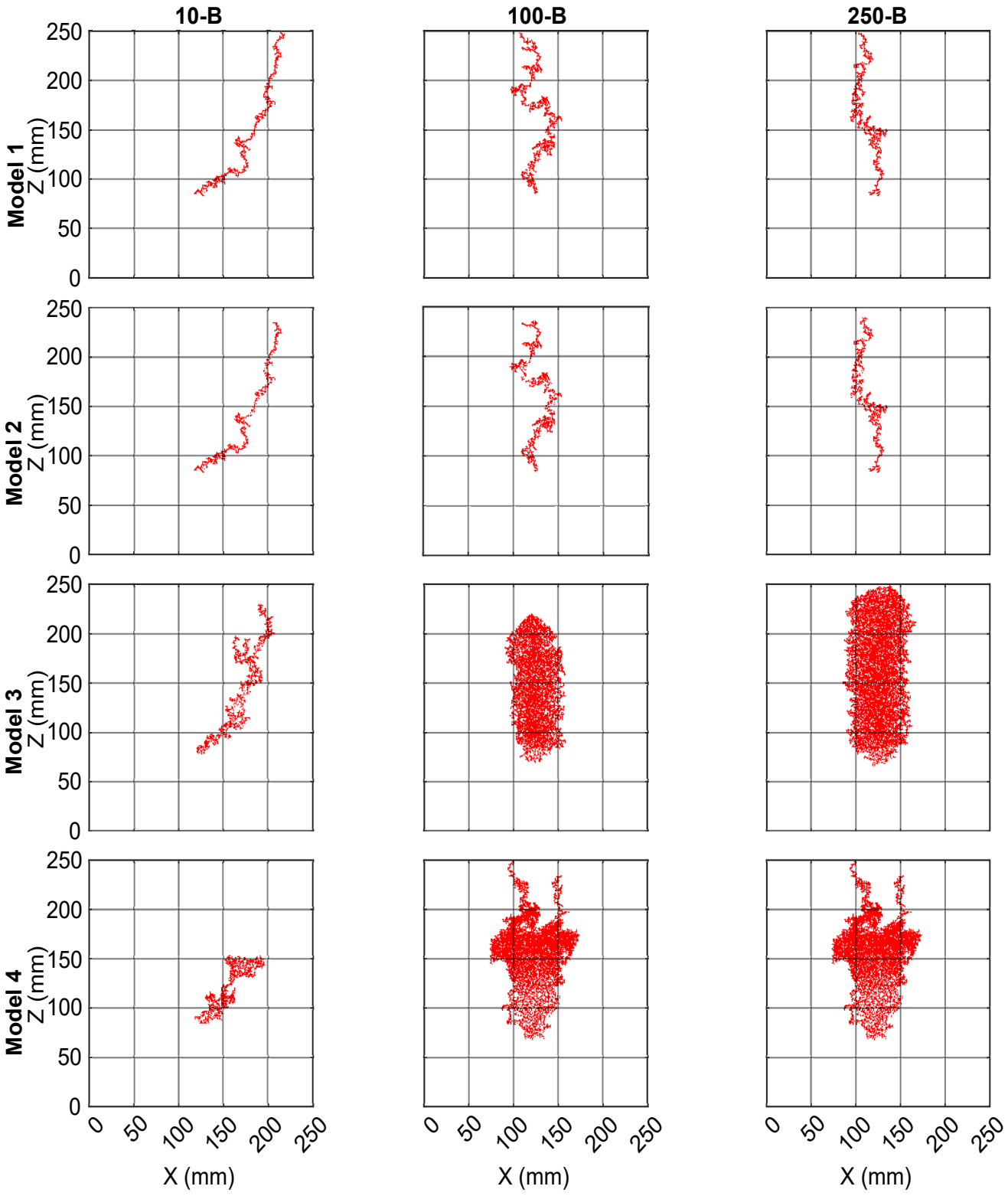


**Figure S3.** Model images for the different model versions with the best fit to non-blurred experimental images (with highest Jaccard value) from experiment no. 10-B, 100-B and 250-B. Row 1, Row 2, Row 3 and Row 4 correspond to Model 1, Model 2, Model 3 and Model 4, respectively.

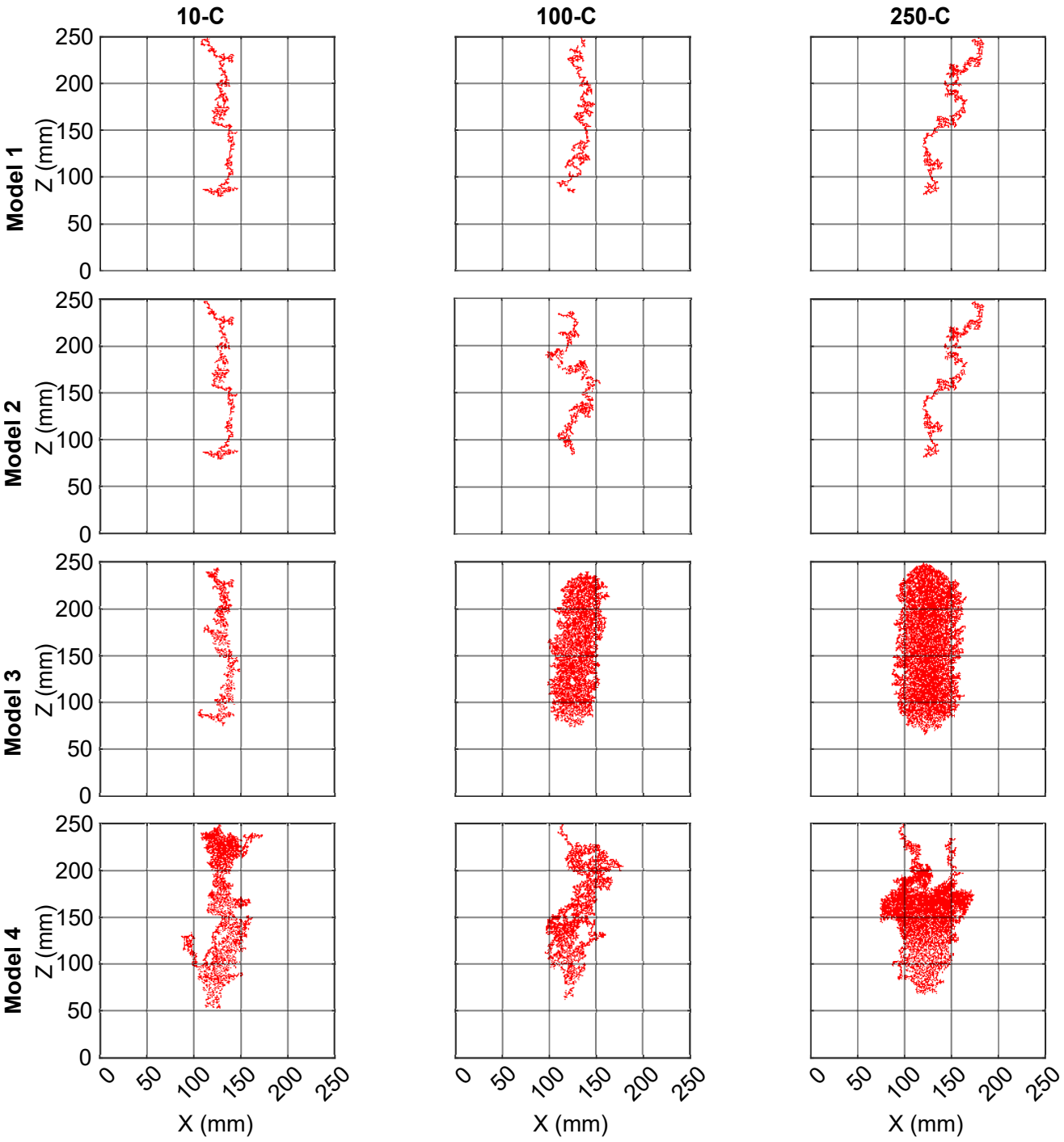


**Figure S4.** Model images for the different model versions with the best fit to non-blurred experimental images (with highest Jaccard value) from experiment no. 10-C, 100-C and 250-C. Row 1, Row 2, Row 3 and Row 4 correspond to Model 1, Model 2, Model 3 and Model 4, respectively.

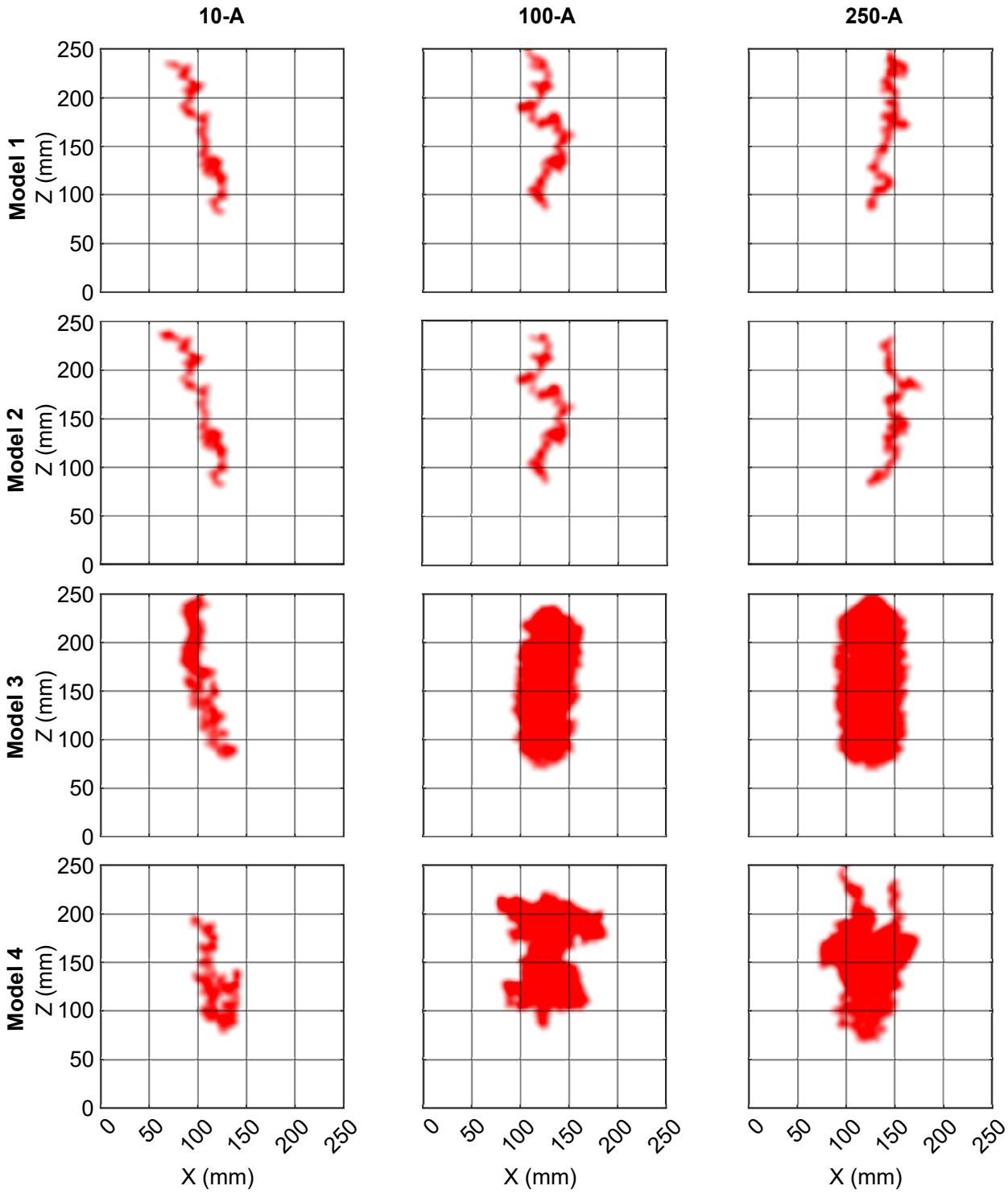


**Figure S5.** Model images for the different model versions with the best fit to blurred experimental images (with highest Diffused Jaccard (low) value) from experiment no. 10-A, 100-A and 250-A. Row 1, Row 2, Row 3 and Row 4 correspond to Model 1, Model 2, Model 3 and Model 4, respectively.

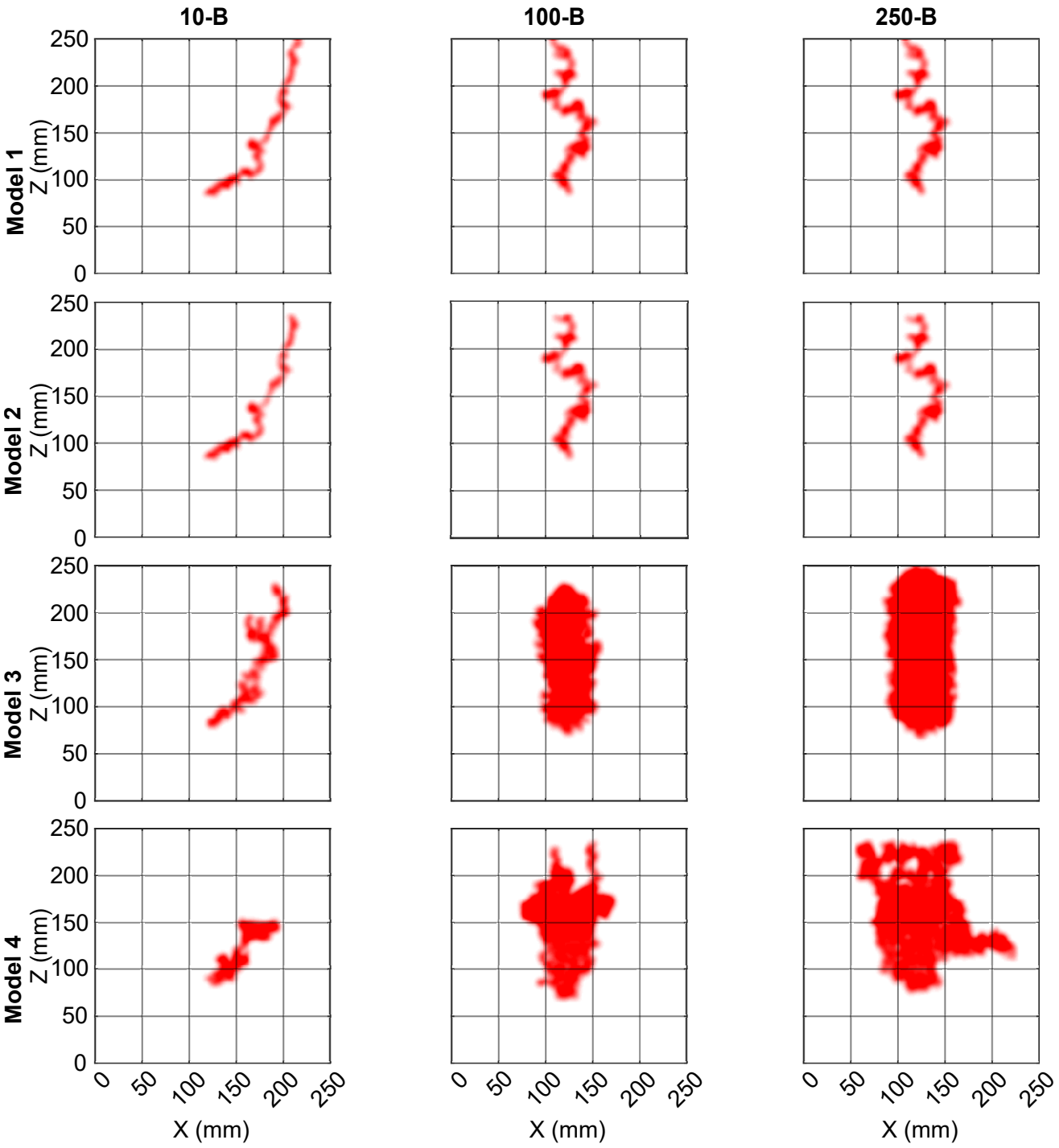


**Figure S6.** Model images for the different model versions with the best fit to blurred experimental images (with highest Diffused Jaccard (low) value) from experiment no. 10-B, 100-B and 250-B. Row 1, Row 2, Row 3 and Row 4 correspond to Model 1, Model 2, Model 3 and Model 4, respectively.

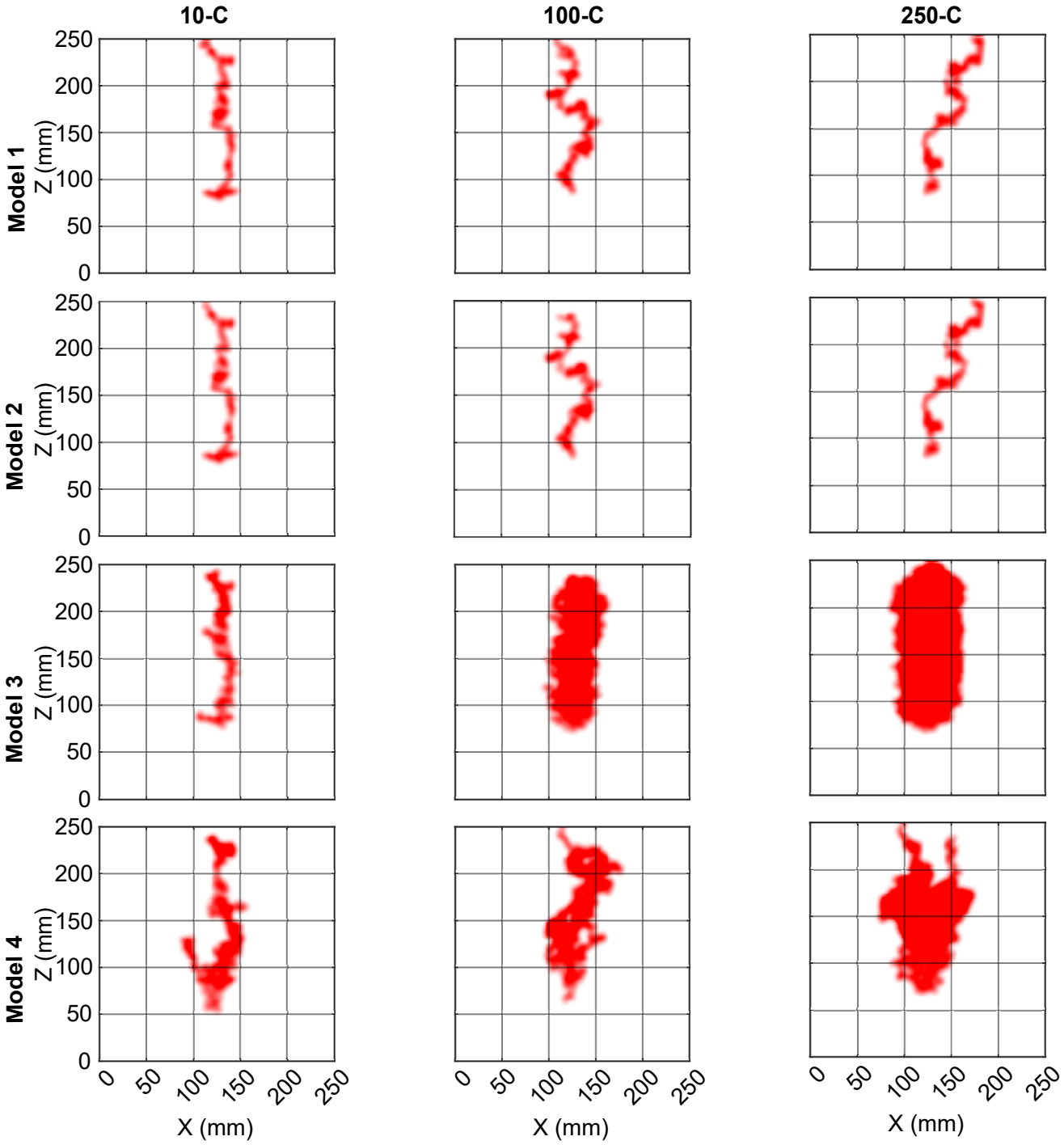


**Figure S7.** Model images for the different model versions with the best fit to blurred experimental images (with highest Diffused Jaccard (low) value) from experiment no. 10-C, 100-C and 250-C. Row 1, Row 2, Row 3 and Row 4 correspond to Model 1, Model 2, Model 3 and Model 4, respectively.

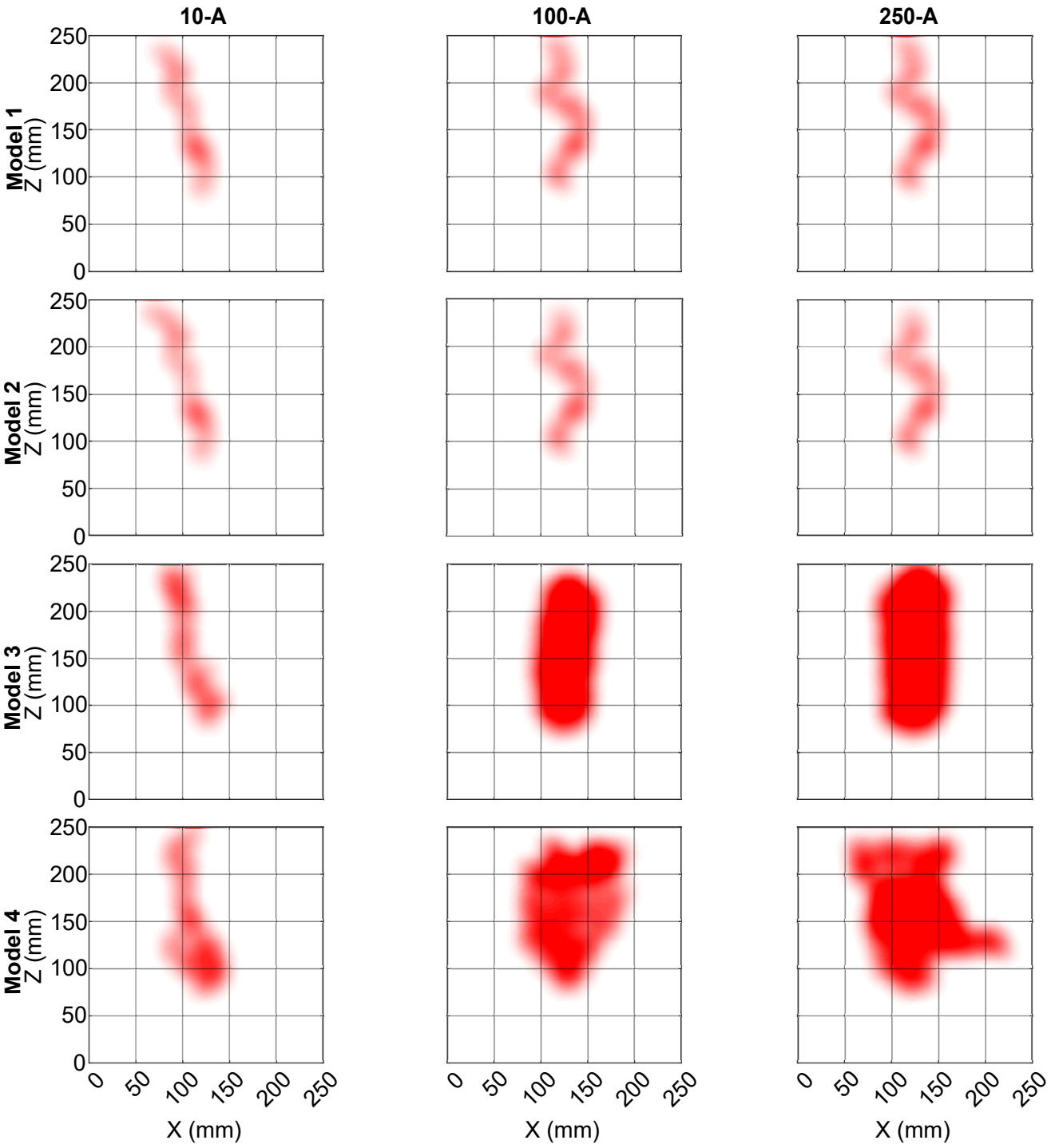


**Figure S8.** Model images for the different model versions with the best fit to blurred experimental images (with highest Diffused Jaccard (med) value) from experiment no. 10-A, 100-A and 250-A. Row 1, Row 2, Row 3 and Row 4 correspond to Model 1, Model 2, Model 3 and Model 4, respectively.

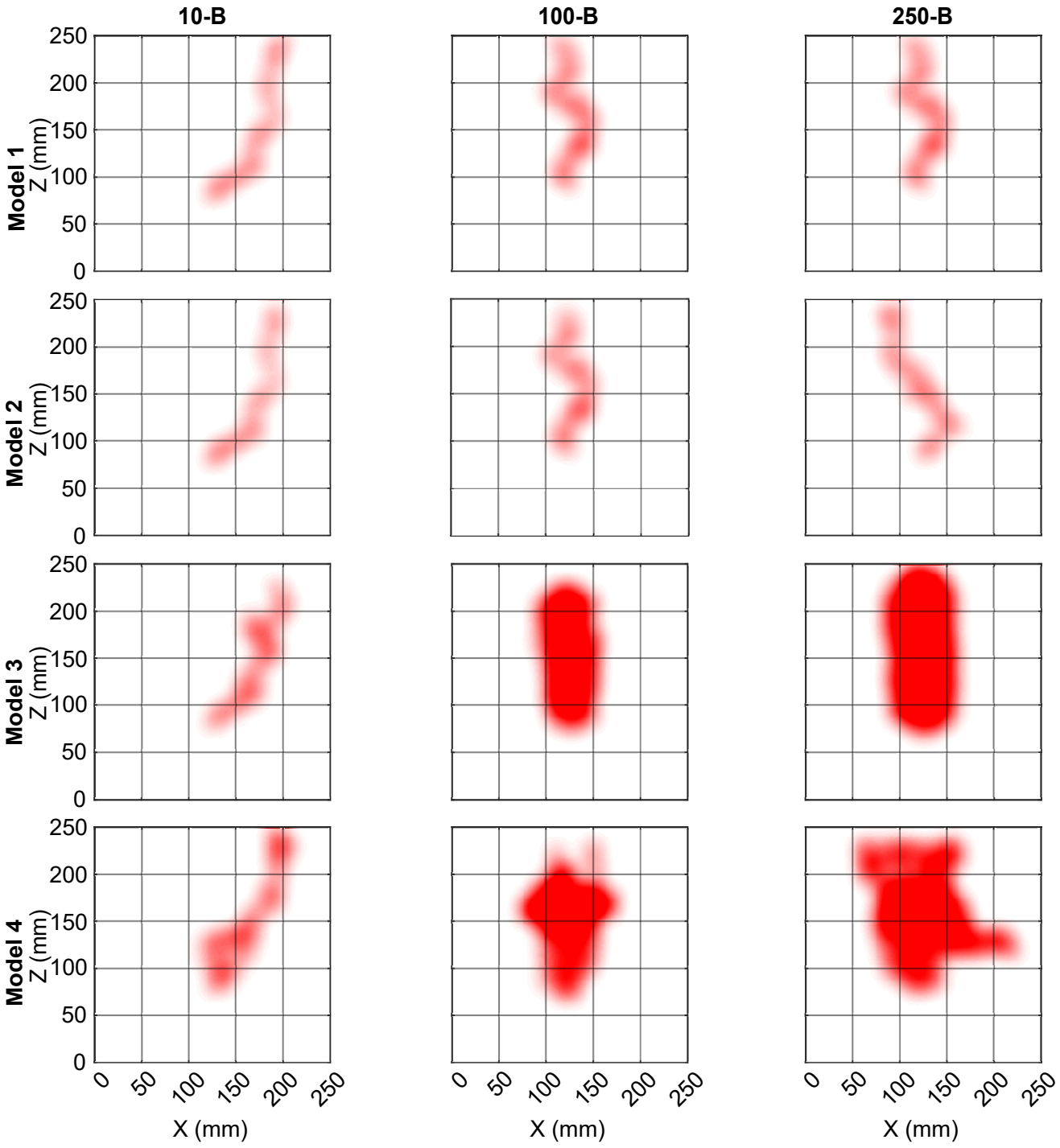


**Figure S9.** Model images for the different model versions with the best fit to blurred experimental images (with highest Diffused Jaccard (med) value) from experiment no. 10-B, 100-B and 250-B. Row 1, Row 2, Row 3 and Row 4 correspond to Model 1, Model 2, Model 3 and Model 4, respectively.

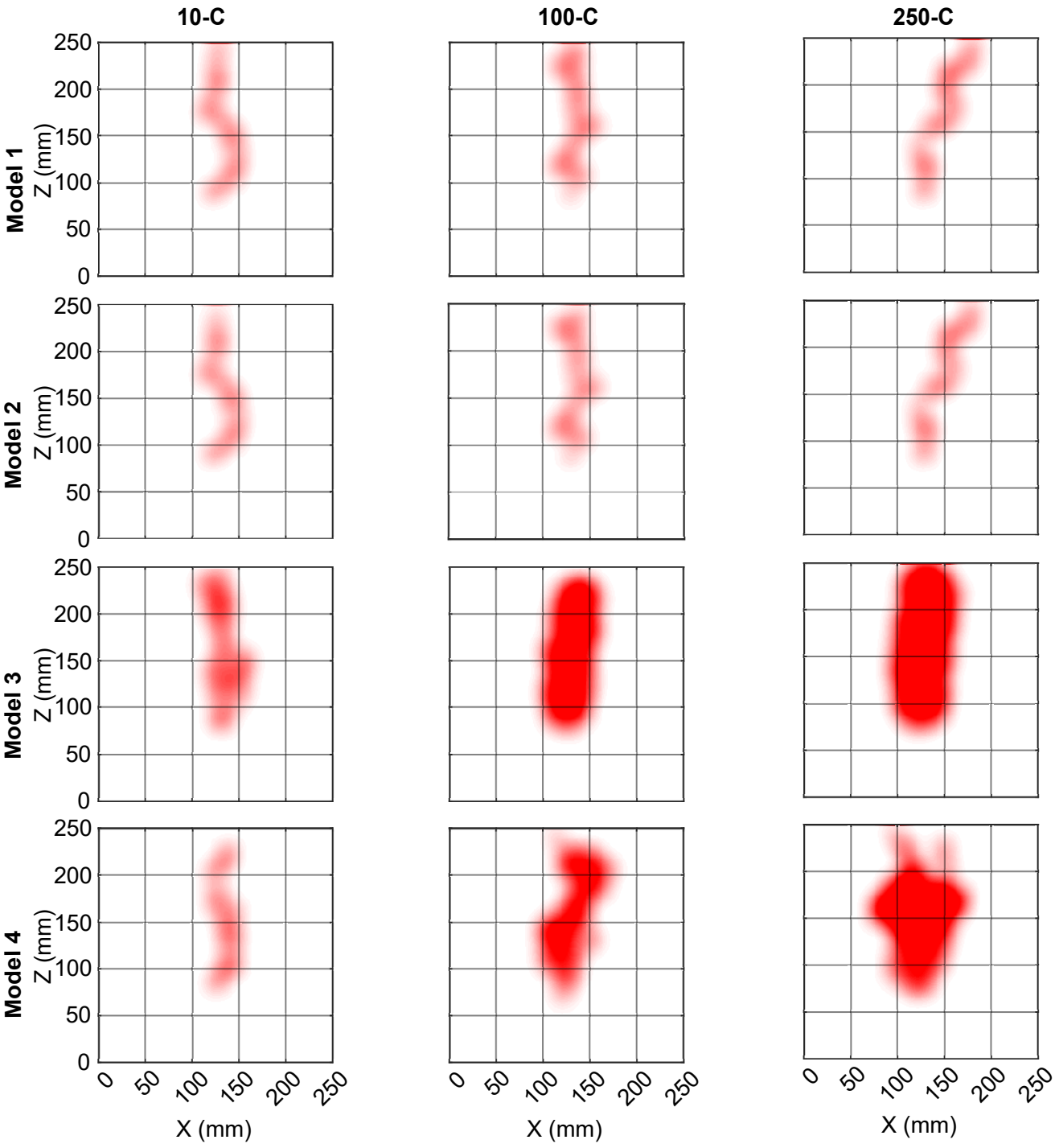


**Figure S10.** Model images for the different model versions with the best fit to blurred experimental images (with highest Diffused Jaccard (med) value) from experiment no. 10-C, 100-C and 250-C. Row 1, Row 2, Row 3 and Row 4 correspond to Model 1, Model 2, Model 3 and Model 4, respectively.

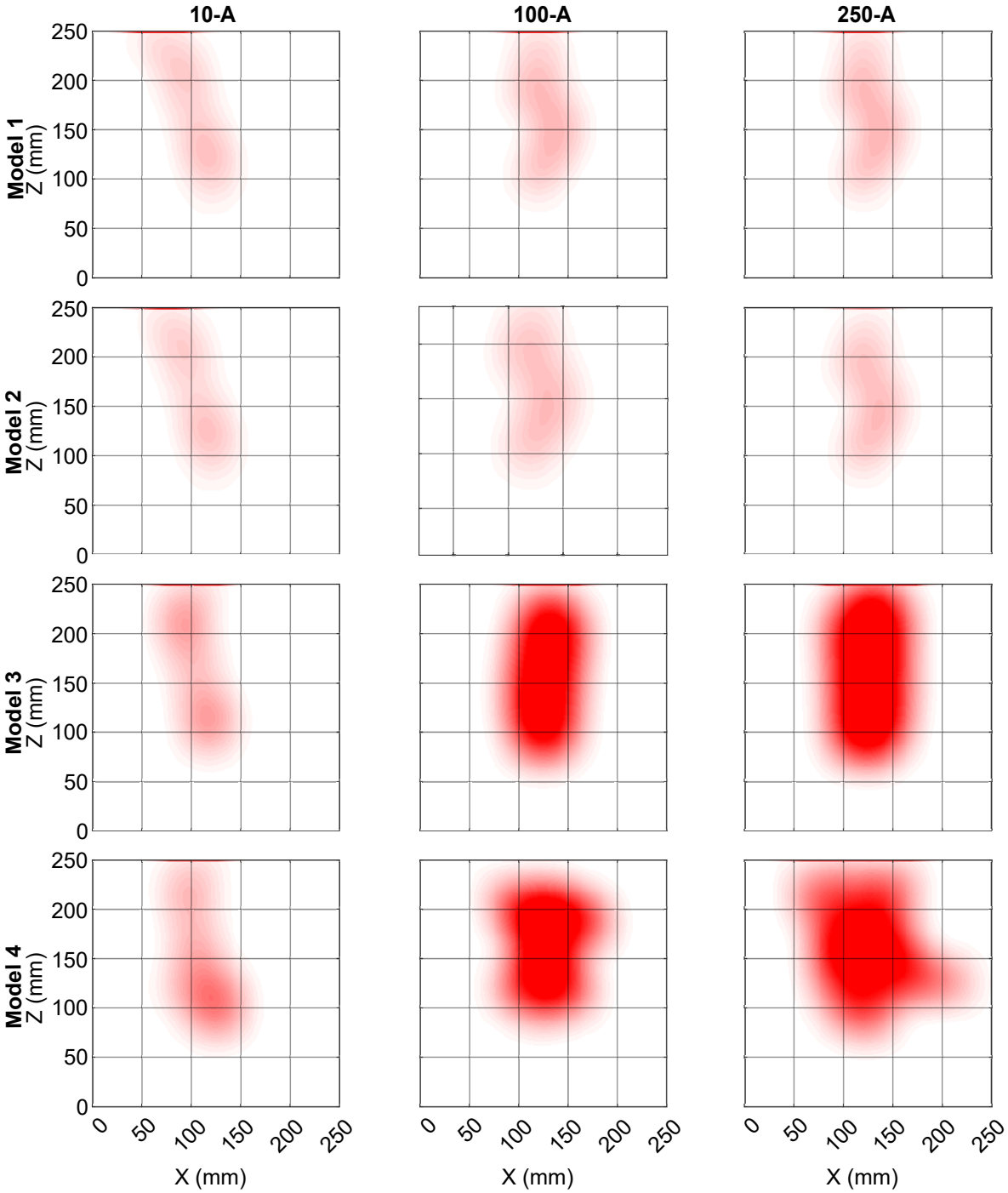


**Figure S11.** Model images for the different model versions with the best fit to blurred experimental images (with highest Diffused Jaccard (high) value) from experiment no. 10-A, 100-A and 250-A. Row 1, Row 2, Row 3 and Row 4 correspond to Model 1, Model 2, Model 3 and Model 4, respectively.

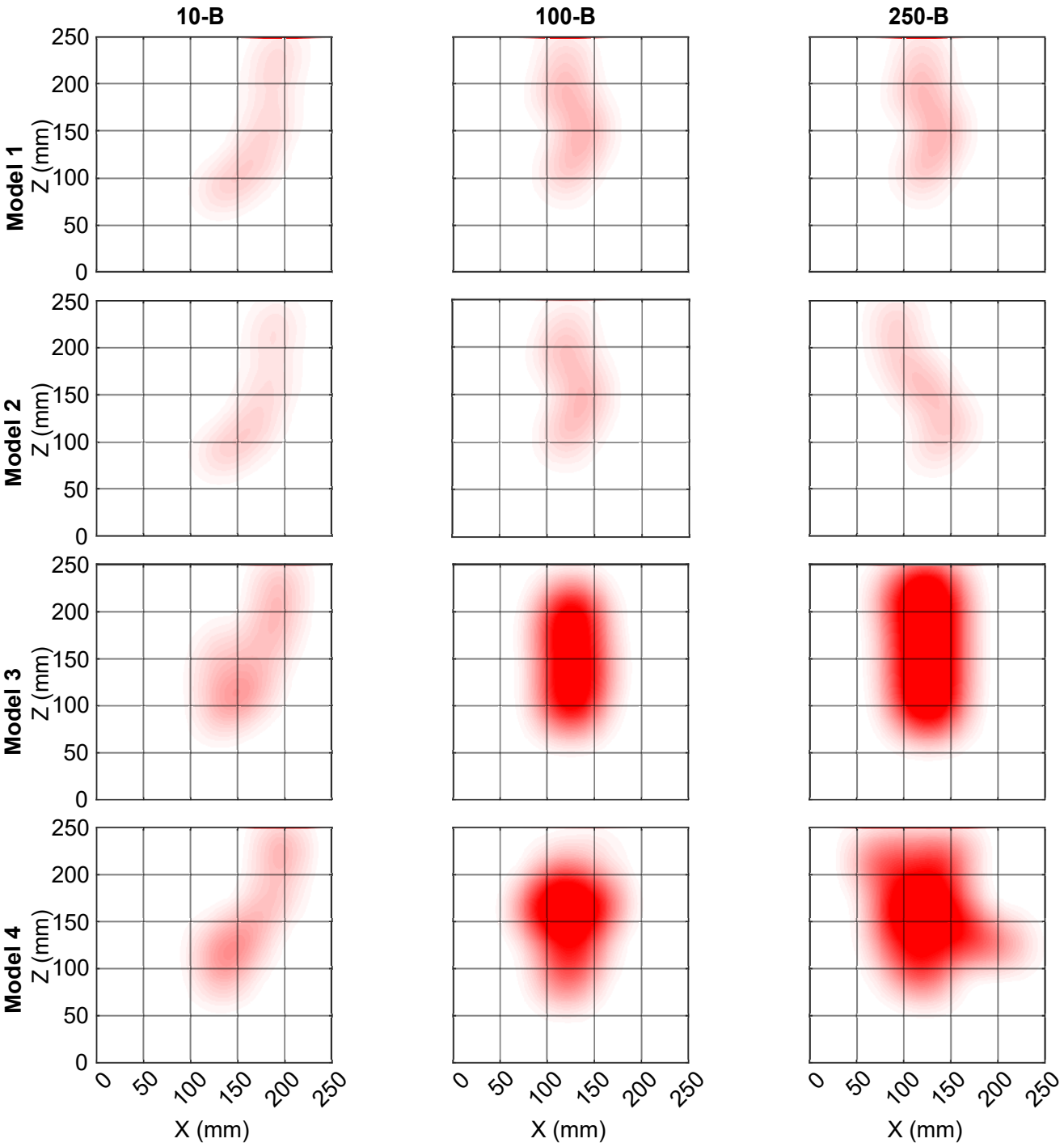


**Figure S12.** Model images for the different model versions with the best fit to blurred experimental images (with highest Diffused Jaccard (high) value) from experiment no. 10-B, 100-B and 250-B. Row 1, Row 2, Row 3 and Row 4 correspond to Model 1, Model 2, Model 3 and Model 4, respectively.

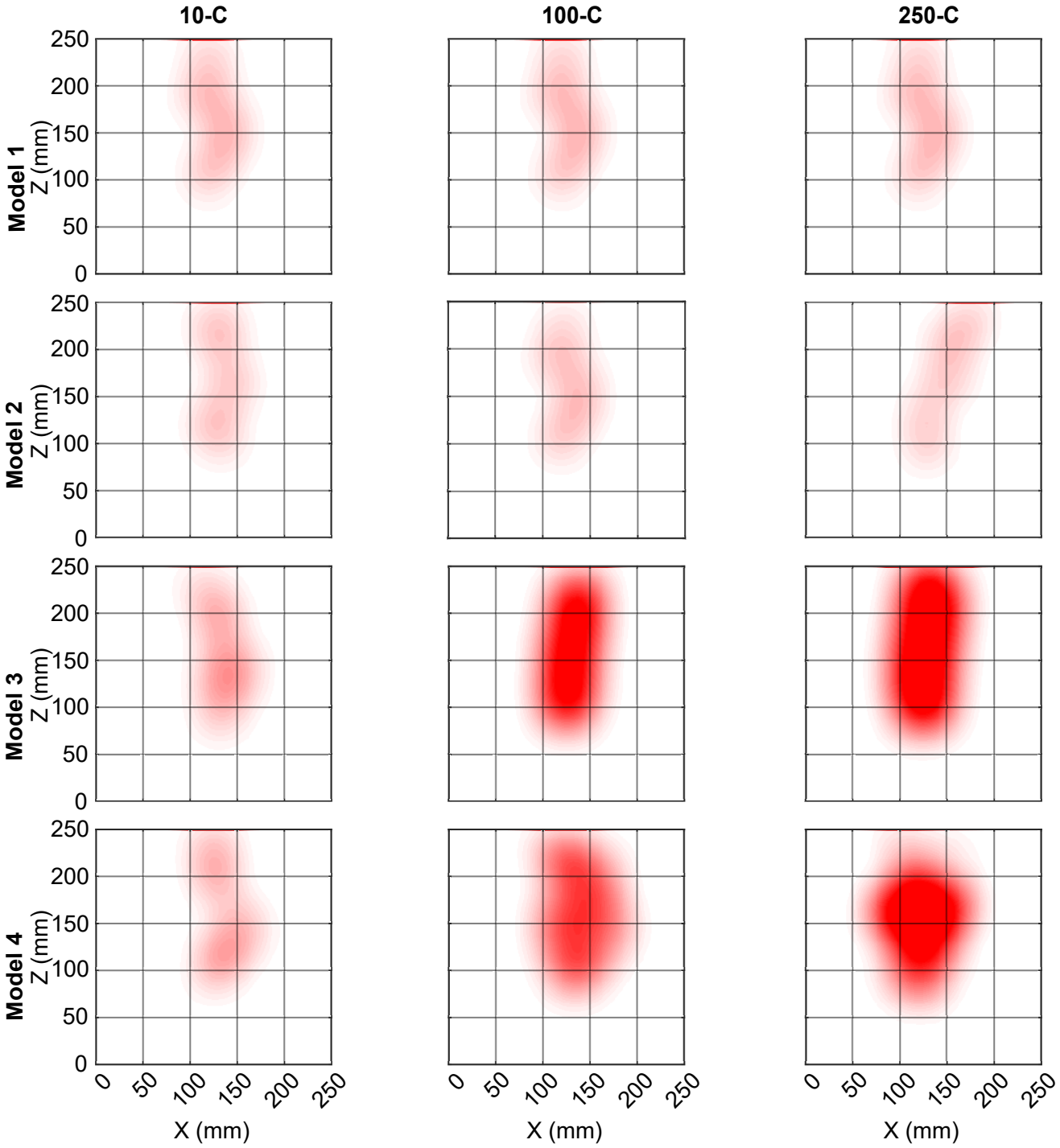


**Figure S13.** Model images for the different model versions with the best fit to blurred experimental images (with highest Diffused Jaccard (high) value) from experiment no. 10-C, 100-C and 250-C. Row 1, Row 2, Row 3 and Row 4 correspond to Model 1, Model 2, Model 3 and Model 4, respectively.